Numerical study of the THM effects on the near-field safety of a hypothetical nuclear waste repository - BMT1 of the DECOVALEX III project. Part 1: Conceptualization and characterization of the problems and summary of results

M. Chijimatsu, T.S. Nguyen, L. Jing, J. de Jonge, M. Kohlmeier, A. Millard, A. Rejeb, J. Rutqvist, M. Souley, Y. Sugita

▶ **To cite this version:**

M. Chijimatsu, T.S. Nguyen, L. Jing, J. de Jonge, M. Kohlmeier, et al.. Numerical study of the THM effects on the near-field safety of a hypothetical nuclear waste repository - BMT1 of the DECOVALEX III project. Part 1: Conceptualization and characterization of the problems and summary of results. International Journal of Rock Mechanics and Mining Sciences, 2005, 42, pp.720-730. 10.1016/j.ijrmms.2005.03.010 . ineris-00175382

HAL Id: ineris-00175382

https://ineris.hal.science/ineris-00175382

Submitted on 1 Oct 2007

HAL is a multi-disciplinary open access archive for the deposit and dissemination of scientific research documents, whether they are published or not. The documents may come from teaching and research institutions in France or abroad, or from public or private research centers.

L'archive ouverte pluridisciplinaire **HAL**, est destinée au dépôt et à la diffusion de documents scientifiques de niveau recherche, publiés ou non, émanant des établissements d'enseignement et de recherche français ou étrangers, des laboratoires publics ou privés.

Numerical study of the THM effects on the near-field safety of a hypothetical nuclear waste repository—BMT1 of the DECOVALEX III project. Part 1: Conceptualization and characterization of the problems and summary of results

M. Chijimatsu (1), T.S. Nguyen (2), L. Jing (3), J. De Jonge (4), M. Kohlmeier (5), A. Millard (6), A. Rejeb (7), J. Rutqvist (8), M. Souley (9) and Y. Sugita (10)

(1) Hazama Corporation, 2-5-5, Toranomon, Minato-ku, Tokyo 105-8479, Japan
(2) Canadian Nuclear Safety Commission (CNSC), Ottawa, Canada
(3) Royal Institute of Technology (KTH), Stockholm, Sweden
(4) University of Tuebingen, Tuebingen, Germany
(1) University of Hannover, Hannover, Germany
(5) Commissariat a l'Energie Atomique (CEA), Paris, France
(6) Institut de Radioprotection et de Sûreté Nucléaire (IRSN), Paris, France
(7) Lawrence Berkeley National Laboratory (LBNL), Berkeley, USA
(8) INERIS-LAEGO, Ecole des Mines de Nancy, Nancy, France
(9) Japan Nuclear Cycle Development Institute (JNC), Ibaraki, Japan

Abstract

Geological disposal of the spent nuclear fuel often uses the concept of multiple barrier systems. In order to predict the performance of these barriers, mathematical models have been developed, verified and validated against analytical solutions, laboratory tests and field experiments within the international DECOVALEX III project. These models in general consider the full coupling of thermal (T), hydraulic (H) and mechanical (M) processes that would prevail in the geological media around the repository. For Bench Mark Test no. 1 (BMT1) of the DECOVALEX III project, seven multinational research teams studied the implications of coupled THM processes on the safety of a hypothetical nuclear waste repository at the near-field and are presented in three accompanying papers in this issue. This paper is the first of the three companion papers, which provides the conceptualization and characterization of the BMT1 as well as some general conclusions based on the findings of the numerical studies. It also shows the process of building confidence in the mathematical models by calibration with a reference T–H–M experiment with realistic rock mass conditions and bentonite properties and measured outputs of thermal, hydraulic and mechanical variables.

Keywords: Thermo-hydro-mechanical couplings; Performance assessment; Radioactive wastes

1. Introduction

The DECOVALEX III project has two main objectives. The first objective is the validation of mathematical models and computer codes by validating against large-scale experiments. The second objective is to determine the relevance of THM processes on the safety of nuclear waste repositories. To achieve the second objective, hypothetical benchmark test problems with realistic geological background and material models/properties were proposed, where effects of THM couplings with typical repository designs, engineered barriers and host rocks are examined. The study on the benchmark problem, Bench Mark Test no. 1 (BMT1), as presented in the three papers in this special issue looks at the implications of coupled THM processes on the near-field performance of a repository with different characterizations of the fractured rocks.

The performance of a nuclear waste repository is dependent on two main components:

(i) the groundwater flow field since groundwater is the main agent of contaminant transport from the repository to the biosphere and

(ii) the structural integrity of the engineered and geological barriers.

The performance assessment (PA) of a repository is often performed with probabilistic approaches using computer codes, with Monte-Carlo simulations. Typically, thousands of runs are performed in order to estimate the probabilistic distributions of radionuclide doses to potential receptors. It is therefore necessary to simplify the processes of contaminant migration in different barriers. The analyses for the aspects of rock mechanics aspects, the engineered barriers and the hydrogeology usually provide information on the structural integrity of the rock mass and performance of the engineered barriers and the groundwater flow field. This information is then synthesized and simplified for defining the models for PA. At present, the above information are usually provided separately, without considering the couplings between the thermal, mechanical (implication on structural integrity) and hydraulic processes (implications on flow field).

In the benchmark problem BMT1 of DECOVALEX III project, we performed scoping calculations in order to determine how the coupled processes could influence the permeability and flow fields, as well as the structural integrity of the geological and engineered barriers in the near-field of a typical repository.

This present paper is the first of three companion papers on BMT1 of DECOVALEX III. In this paper we introduce the subject, the conceptualization, characterization and technical definition of the problem and summarize the main conclusions.

BMT1 is divided into three phases that will be discussed in more detail in the three companion papers:

(i) *Phase A:* Development and validation of THM models and computer codes through calibration against the measured output from an in situ THM experiment at the Kamaishi mine in Japan. The objective of the calibration is to build confidence in the models and codes used by different research teams in the subsequent scoping calculations. The result of this phase is described in this paper.

(ii) *Phase B:* Scoping calculations for a hypothetical repository in a continuous and homogeneous rock. The bentonite as an engineered barrier in the hypothetical repository is the same as the one used in the THM experiment at the Kamaishi mine. However, the permeability and strength characteristics of the rock mass are based on data obtained from the sparsely fractured rock of the Canadian Shield. The results are reported in [1].

(iii) *Phase C:* Scoping calculations for a hypothetical repository similar to the one in Phase B, but with the additional consideration of discrete fractures intersecting the repository. The results are presented in [2].

2. General definition of the BMT1 problem

The BMT1 concerns a hypothetical nuclear waste repository in a granitic rock formation at a depth of 1000 m [3] with reference to an experimental site at the Kamaishi Mine in Japan, where tunnels were excavated down to a depth of 600 m and a variety of hydraulic, mechanical and geochemical tests have been performed as shown in Fig. 1 [4]. Of particular relevance to the assessment proposed in BMT1 is a THM experiment probing the near-field behaviour of the rock mass and buffer around a single waste container as shown in Fig. 2 [5]. The type of bentonite used in the above experiment and the dimensions of the experimental borehole are comparable with the parameters of the conceptual design of the repository as shown in Fig. 3 [3].

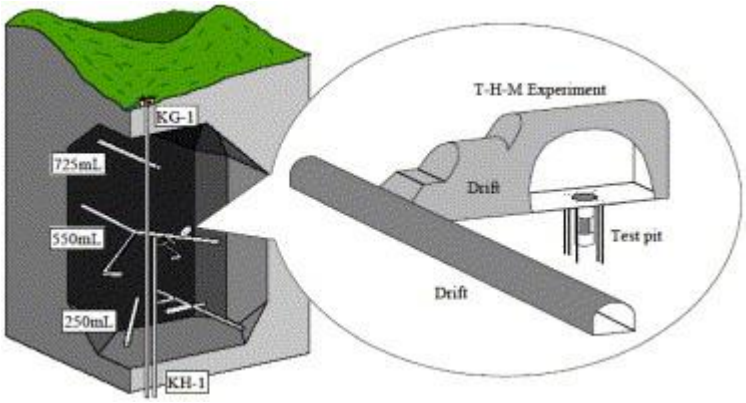

Fig. 1. Underground experimental site.

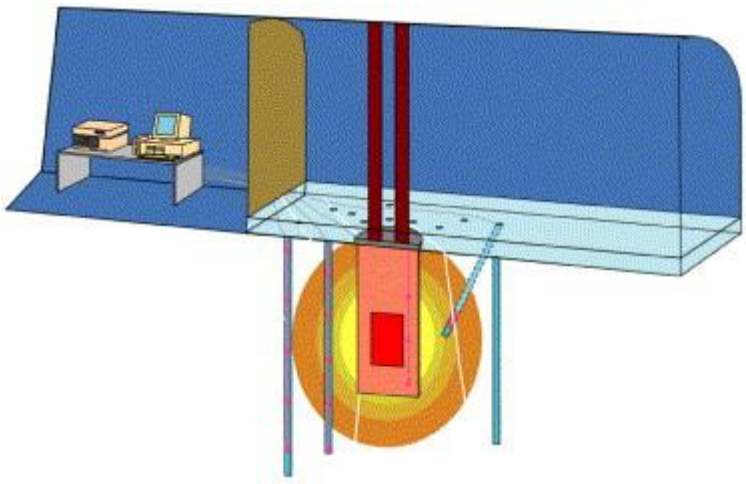

Fig. 2. Schematic view of the THM experiment at the Kamaishi mine.

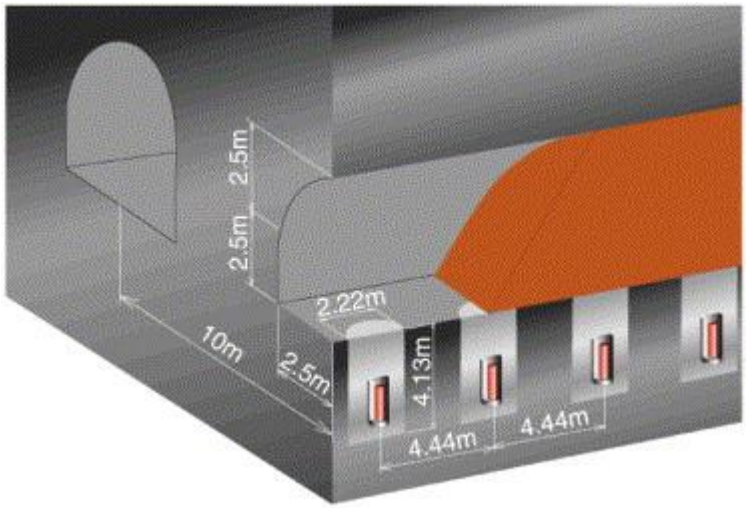

Fig. 3. Conceptual design of the hypothetical repository in Japan.

The conceptual design of the repository, as shown in Fig. 3 [3], consists of a series of parallel tunnels, where the wastes would be emplaced in vertical boreholes excavated in the floors of the tunnels. The centreline distance between the adjacent tunnels is 10 m and the centreline distance between adjacent vertical boreholes for waste emplacement is 4.44 m. The depth of each borehole is 4.13 m and the diameter is 2.22 m. The overpack for vitrified wastes would be emplaced into the boreholes, and a bentonite buffer material would be compacted around the overpack. The tunnels would also be backfilled with a mixture of gravel and clay after waste emplacement.

Performance assessment of the hypothetical repository will need answers to the following questions from numerical modelling of the THM processes:

(1) What is the temperature evolution in the near-field ?

(2) How long would it take for the buffer to resaturate ?

(3) What are the stresses on the overpack and the buffer ? Will they be structurally stable ?

(4) How will the permeability and the flow field of the rock mass in the near-field evolve ?

(5) Is there a potential of rock mass failure in the near-field ?

(6) Last but not least, is the THM coupling important and which coupling can be ignored ?

The THM mathematical models, implemented in computer codes, will be needed as tools to address the questions raised above. The work is divided into two phases:

(1) Calibration of the code with the T–H–M experiment performed at the 550 m-level gallery at the experimental site, illustrated in Fig. 1. This step is considered as crucial in building confidence in the codes' capabilities to take into account the main physical processes.

(2) Use of the codes to perform scoping calculations of the near-field T–H–M behaviour of the generic design shown in Fig. 3, in order to address the above PA-related questions.

The hypothetical repository defined above has rather composite features: it is in fact based on one of the Japanese conceptual designs as shown in Fig. 3 [3]. The buffer material is the same pure bentonite [6] used in a real THM experiment [5] at the Kamaishi mine in Japan as shown in Fig. 1. The in situ state of stress and the natural thermal gradient are also based on Japanese geological data. However, the rock mass properties in terms of strength and permeability are based on typical Canadian Shield's data.

3. Calibration with the in situ T–H–M field experiment at the Kamaishi mine

The confidence building in the mathematical models and computer codes was conducted by calibration with an in situ T–H–M experiment for realistic rock mass conditions and bentonite properties using measured outputs of thermal, hydraulic and mechanical variables carried out, defined as phase A of BMT1. The experiment chosen for this work is the coupled in situ THM experiment at the Kamaishi mine in Japan. Five research teams as shown in Table 1 simulated the in situ THM experiment. A number of improvements to previous works performed during DECOVALEX II [7] and [8] were suggested and tested in this study. The suggested improvements were tested using a simplified axisymmetric model of the in situ THM experiment.

Table 1. Research team and simulation code

Research team	**Simulation code**
CNSC (Canada)	FRACON
JNC (Japan)	THAMES
KTH/SKI (Sweden)	ROCMAS
CEA/IRSN (France)	Castem 2000
INERIS/ANDRA (France)	FLAC

3.1. Outline of the Kamaishi in situ T–H–M experiment

A schematic view of the Kamaishi in situ THM experiment is shown in Fig. 2 [5]. A granulated bentonite was compacted directly into the test pit, by layers of 10 cm thickness. The initial water content (by weight) of the bentonite was 15 %. A heater was installed in the test pit, surrounded by the bentonite. When bentonite was compacted within the last 50 cm of the pit, a concrete lid was installed for the remaining part. This lid was restrained by vertical steel bars connected to the ceiling of the drift, in order to restrict the vertical movements. A 40-cm-deep water pool was then constructed on the floor of the test drift. The temperature at the centre of the heater was maintained at 100 °C during a heating phase of 258 days. The heater was then turned off, and the natural cooling phase took place for approximately 180 days. Measurements from the installed sensors were recorded during the complete heating and cooling phases.

3.2. The calibration against the in situ THM experiment using a simplified axisymmetric model

A simplified calibration test case of the in situ experiment is proposed and defined below. The case focuses on the THM behaviour along a radial line (with a radial distance "r" as the coordinate) from the centre of the heater, with the axisymmetric geometry as shown in Fig. 4.

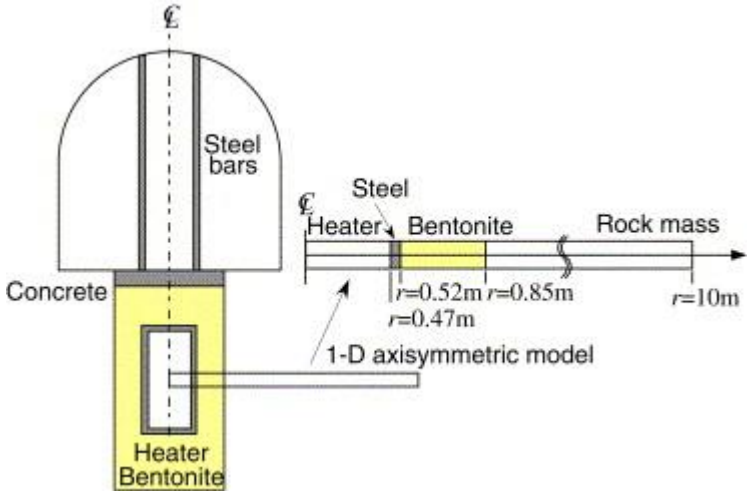

Fig. 4. Geometry of the simplified axisymmetric model.

The desired output parameters are as follows: T is the temperature (°C); u the radial displacement (m): p the pore pressure (Pa); ω the water content by weight (%); σ the total radial stress (Pa); ε_ρ and ε_τ the radial and tangential strains, respectively. Time histories of these output parameters were calculated for both the heating and cooling phases.

The boundary conditions are defined as follows:

> *At r = 0.47 m:* T = 100°C (heating) and free temperature (cooling), free displacement, impermeable.
>
> *At r = 10 m:* T = 12 °C, u = 0, (equivalent to 0.4 m of water).

The initial conditions are as follows:

> T = 12 °C and zero displacements and stresses everywhere; p = 3.9 kPa in the rock; ω =15 % in the bentonite.

3.3. Physical process and constituent models in different codes applied for BMT1A study

3.3.1. The CNSC model

In the FRACON [7] code developed and used by the CNSC for the BMT1 study, the bentonite was assumed to be a poroelastic continuum of generalized Biot's type. The physical processes considered are heat conduction, pore water flow in saturated/unsaturated porous media, vapour flow driven by temperature gradient and mechanical deformation of the bentonite skeleton. These processes are described by the following governing equations.

The energy conservation equation is given as:

$$\frac{\partial}{\partial x_i}\left(\kappa_{ij}\frac{\partial T}{\partial x_j}\right)+q=\rho C\frac{\partial T}{\partial t}, \tag{1}$$

where T is the temperature, κ_{ij} the heat conductivity tensor, q the heat source (or sink), ρ the bulk density and C the specific heat.

The continuity equation of groundwater is given as:

$$\begin{aligned}&\frac{\partial}{\partial x_i}\left[\frac{\rho_w k_{ij}K_r}{\mu}\left(\frac{\partial P}{\partial x_j}+\rho_w g_i\right)\right]-\frac{\partial}{\partial x_i}\left(D_{Tv}\frac{\partial T}{\partial x_i}\right)\\&\quad+\rho_w n\frac{dS_r}{dP}\frac{\partial P}{\partial t}-S_r B_w\frac{\partial P}{\partial t}-\rho_w S_r\frac{\partial}{\partial t}\left(\frac{\partial u_r}{\partial x_r}\right)\\&\quad+\rho_w S_r\left[n\beta_w+(1-n)\beta_s\right]\frac{\partial T}{\partial t}=0,\end{aligned} \tag{2}$$

where k_{ij} is the saturated permeability tensor, K_r the non-dimensional relative permeability of the unsaturated medium, S_r the degree of saturation, μ the water viscosity, ρ_w the water density, D_{Tv} the thermal diffusivity of the vapour, n the porosity and B_w the coefficient of water compressibility, respectively. The symbols β_w and β_s are the thermal expansion coefficients of water and solid, respectively. P is the water pressure.

The equilibrium equation is given as:

$$\begin{aligned}&G\frac{\partial^2 u_i}{\partial x_j\partial x_j}+(G+\lambda)\frac{\partial^2 u_j}{\partial x_i\partial x_j}+\chi(S)\frac{\partial P}{\partial x_i}\\&\quad-\beta K_d\frac{\partial T}{\partial x_i}+F_i=0,\end{aligned} \tag{3}$$

where u_i is the displacement vector, G and λ are Lame's elasticity constants, β the volumetric thermal expansion coefficient of the solid matrix, χ the Bishop's coefficient of effective stress, K_d the bulk modulus and F_i the body force.

3.3.2. The JNC model

The behaviour of the buffer material is influenced by the interdependence of thermal, hydraulic and mechanical phenomena. To simulate the water/vapour movement and heat-induced water movement, the continuity equation used in the extended THAMES [7] code is as follows:

$$\left\{\xi\rho_{\mathrm{w}}D_{\theta}\frac{\partial\theta}{\partial\psi}(h_{,i}-z_{,i})+(1-\xi)\frac{\rho_{\mathrm{w}}^{2}gK}{\mu_{l}}h_{,i}\right\}$$
$$+\left\{\rho_{\mathrm{w}}D_{\mathrm{Tv}}T_{,i}\right\}_{,i}-\rho_{\mathrm{wo}}nS_{\mathrm{r}}\rho_{\mathrm{w}}g\beta_{\mathrm{P}}\frac{\partial h}{\partial t}-\rho_{\mathrm{w}}\frac{\partial\theta}{\partial\psi}\frac{\partial h}{\partial t}$$
$$-\rho_{\mathrm{w}}S_{\mathrm{r}}\frac{\partial u_{i,i}}{\partial t}+\rho_{\mathrm{wo}}nS_{\mathrm{r}}\beta_{\mathrm{T}}\frac{\partial T}{\partial t}=0, \qquad (4)$$

where D_θ is the isothermal water diffusivity, θ the volumetric water content, ψ the water potential and K the intrinsic permeability. The symbol ξ is the relative saturation parameter so that $\xi = 0$ when the medium is fully saturated and $\xi = 1$ otherwise. μ_l is the viscosity of water, n the porosity, S_r the degree of saturation, β_P the compressibility of water, β_T the thermal expansion coefficient of water and z the elevation head. The variable u_i is the displacement vector, T the temperature, h the total head and t the time. The subscript 0 means the reference state.

The energy conservation equation takes into account the heat transfer by conduction and convection, as well as the energy change by evaporation. The equation is given as

$$(\rho C_{\mathrm{v}})_{\mathrm{m}}\frac{\partial T}{\partial t}+nS_{\mathrm{r}}\rho_{\mathrm{w}}C_{\mathrm{vl}}V_{li}T_{,i}-K_{\mathrm{Tm}}T_{,ii}$$
$$+L\left\{D_{\theta\mathrm{v}}\frac{\partial\theta}{\partial\psi}(h_{,i}-z_{,i})\right\}_{,i}+nS_{\mathrm{r}}T\frac{\beta_{\mathrm{T}}}{\beta_{\mathrm{P}}}$$
$$\left\{\xi D_{\theta}\frac{\partial\theta}{\partial\psi}(h_{,i}-z_{,i})+(1-\xi)\frac{\rho_{\mathrm{w}}gK}{\mu_{l}}h_{,i}+D_{\mathrm{T}}T_{,i}\right\}_{,i}$$
$$+\frac{1}{2}(1-n)\beta T\frac{\partial}{\partial t}(u_{i,j}+u_{j,i})\delta_{ij}=0, \qquad (5)$$

where (?Cv)m is the specific heat of the material consisting of water and the solid particles, Cvl the specific heat of water, Vli the velocity vector of water, KTm the thermal conductivity of the medium consisting of water and the solid particles, L the latent heat of vaporization per unit volume and D?v the vapour diffusivity.
The equilibrium equation takes the swelling behaviour of the partially saturated bentonite into account and is written as

$$\left[\tfrac{1}{2}C_{ijkl}(u_{k,l}+u_{l,k})-F\pi\delta_{ij}-\beta\delta_{ij}(T-T_{\mathrm{o}})\right.$$
$$\left.+\chi\delta_{ij}\rho_{\mathrm{w}}g(h-z)\right]+\rho b_{i}=0, \qquad (6)$$

where C_{ijkl} is the elastic matrix, ρ the density of the medium and b_i the body force. χ is the parameter for the effective stress, $\chi = 0$ for the unsaturated zone and $\chi = 1$ for the saturated zone. The symbol F is the coefficient relating to the swelling pressure process and $\beta=(3G+2\lambda)$as, where as is the thermal expansion coefficient of solid particles.

3.3.3. The KTH/SKI model

The governing equations of ROCKMAS [7] are as follows. The mass conservation of water and vapour, energy conservation and momentum conservation equations are given as:

$$\begin{aligned}
&\alpha\left[S_{\mathrm{r}}\rho_{\mathrm{w}}+(1-S_{\mathrm{r}})\rho_{\mathrm{v}}\right]\\
&\quad+\left[nS_{\mathrm{r}}\rho_{\mathrm{w}}^{0}\beta_{\mathrm{p}}+n(\rho_{\mathrm{w}}-\rho_{\mathrm{v}})C_{\mathrm{s}}+n(1-S_{\mathrm{r}})\frac{\rho_{\mathrm{v}}}{\rho_{\mathrm{w}}RT}\right]\frac{\partial P}{\partial T}\\
&\quad+\left[nS_{\mathrm{r}}\rho_{\mathrm{w}}^{0}\beta_{\mathrm{T}}+n(1-S_{r})\left(h\frac{\partial\rho_{\mathrm{vs}}}{\partial T}+\frac{\rho_{\mathrm{v}}P}{RT^{2}}\right)\right]\frac{\partial T}{\partial t}\\
&=\nabla\cdot\left[\left(\frac{\rho_{\mathrm{w}}k_{\mathrm{w}}}{\mu_{\mathrm{w}}}+D_{\mathrm{Pv}}\right)\nabla P+\frac{\rho_{\mathrm{w}}k_{\mathrm{w}}}{\mu_{\mathrm{w}}}\gamma_{\mathrm{w}}\nabla z\right]\\
&\quad-\nabla\cdot(D_{\mathrm{Tv}}\nabla T),
\end{aligned}\tag{7}$$

$$\begin{aligned}
&\left[(1-n)\rho_{\mathrm{s}}C_{\mathrm{vs}}+\rho_{\mathrm{w}}C_{\mathrm{ws}}nS_{\mathrm{r}}+\rho_{\mathrm{v}}C_{\mathrm{pv}}n(1-S_{\mathrm{r}})\right.\\
&\quad\left.+H_{\mathrm{l}}\left(h\frac{\partial\rho_{\mathrm{vs}}}{\partial T}-\frac{\rho_{\mathrm{v}}P}{RT^{2}}\right)\right]\frac{\partial T}{\partial t}\\
&\quad+\beta T_{0}\frac{\partial e}{\partial t}+\nabla\cdot\left(C_{\mathrm{vw}}q_{\mathrm{w}}^{\mathrm{m}}+C_{\mathrm{pv}}q_{\mathrm{v}}^{\mathrm{m}}\right)\nabla T\\
&=\nabla\cdot\left[(K_{\mathrm{M}}+LD_{\mathrm{Tv}})\cdot\nabla T+LD_{\mathrm{pv}}\nabla P\right]\\
&\quad-H_{2}\frac{\partial(nS_{\mathrm{r}})}{\partial t}-\left(H_{\mathrm{l}}\frac{\rho_{\mathrm{v}}}{\rho_{\mathrm{w}}RT}+H_{2}\frac{\partial(nS_{\mathrm{r}})}{\partial P}\right)\frac{\partial P}{\partial t},
\end{aligned}\tag{8}$$

$$\begin{aligned}
&\frac{\partial}{\partial x_{j}}\left[C_{ijkl}e_{kl}-\delta_{ij}\beta(T-T_{0})-\delta_{ij}\zeta(S_{\mathrm{r}}-S_{\mathrm{r0}})\right.\\
&\quad\left.-\delta_{ij}\alpha S_{\mathrm{r}}\bar{P}\right]+\bar{\rho}_{\mathrm{s}}f=0,
\end{aligned}\tag{9}$$

where α is the Biot's coupling constant, V_w the fluid density by weight, ξ the coefficient of swelling, the average solid mass density, ρ_v the vapour mass density, ρ_{vs} the saturated vapour mass density, C_s the moisture capacity, e the volumetric elastic strain, R the specific gas constant, f the body force per unit mass, k_w the water permeability, K_M the thermal conductivity of solid–fluid mixture, D_v the effective molecular diffusivity of water vapour in air, L the latent heat of vaporization and C_{vs}, C_{vw}, C_{Pv} the volumetric specific heat capacity of solid, water and vapour, respectively.

3.3.4. The IRSN/CEA model

The model that has been implemented in the computer code Castem 2000 [9] for the simulation of coupled THM responses of unsaturated soils is based on the equations governing the evolution of the chosen primary variables, which are the displacements ξ, the liquid water pressure p_l and the temperature T and are obtained from conservation equations together with state laws.

The water mass conservation equation is:

$$\begin{aligned}\frac{\partial}{\partial t}(\rho_l S_l \varphi) &= -\operatorname{div} \underline{q_l} - \operatorname{div} \underline{q_v} \\ &= +\operatorname{div}\left[\frac{K k_{rl} \rho_l}{\eta_l}(\underline{\operatorname{grad}}\ p_l - \rho_l \underline{F})\right] \\ &\quad + \operatorname{div}(D_{T_v}\ \underline{\operatorname{grad}}\ T),\end{aligned} \qquad (10)$$

where K is the intrinsic permeability, k_{rl} the permeability relative to liquid water and η_l the dynamic viscosity of water. Symbol F stands for body forces such as gravity.
The conservation of momentum is written as

$$\operatorname{div} \underline{\underline{\sigma}} + \rho \underline{F} = 0, \qquad (11)$$

where σ stands for the total stress in the porous medium and ρ is its equivalent density.

Finally, the conservation of energy is simply taken in a simplified form:

$$\rho C \frac{\partial T}{\partial t} - \operatorname{div}\left(K_T \cdot \underline{\operatorname{grad}}\ T\right) = q, \qquad (12)$$

where ρC stands for the heat capacity of the equivalent porous medium, K_T is the heat conductivity and q represents a heat source.

The temperature equation is solved separately, whereas the water mass conservation and momentum conservation equations are solved together. Because of the strong non-linearity that is present in these equations, a fully implicit time integration scheme is used.

3.3.5. The INERIS/ANDRA model

The two-phase flow option in FLAC allows numerical modelling of the flow of two immiscible fluids through porous media. Some of these concepts are addressed below.

In a two-phase flow problem, the void space is completely filled by two fluids. One of the fluids (the liquid fluid, identified by the subscript lq) wets the porous medium more than the other (the gas fluid, identified by subscript gz). As a result, the pressure in the non-wetting fluid will be higher than the pressure in the wetting fluid. The pressure difference P_{gz}–P_{lq} is the capillary pressure P_c, which is a function of saturation S_{lq}. Darcy's law is used to describe the flow of each fluid. The effective intrinsic permeability is given as a fraction of the single-fluid intrinsic permeability. The fractions (or relative permeability) are functions of saturation, S_{lq}.

In addition to the mechanical balance of momentum, the mechanical constitutive equations and compatibility equation, some additional equations are used for coupled calculations, as described below.

The transport equations of liquid and gas components are described by Darcy's law:

$$q_i^{\mathrm{lq}} = -k_{ij}^{\mathrm{lq}} \kappa_{\mathrm{r}}^{\mathrm{lq}} \frac{\partial}{\partial xj}(P_{\mathrm{lq}} - \rho_{\mathrm{lq}} g_k x_k),$$
$$q_i^{\mathrm{gz}} = -k_{ij}^{\mathrm{lq}} \kappa_{\mathrm{r}}^{\mathrm{gz}} \frac{\partial}{\partial xj}(P_{\mathrm{gz}} - \rho_{\mathrm{gz}} g_k x_k), \qquad (13)$$

where k_{ij} is the saturated mobility tensor and κ_r the relative permeability for the fluid.

The constitutive equations are:

$$S_{\mathrm{lq}} \frac{\partial P_{\mathrm{lq}}}{\partial t} = -\frac{K_{\mathrm{lq}}}{\phi}\left[\frac{\partial \zeta_{\mathrm{lq}}}{\partial t} - \phi \frac{\partial S_{\mathrm{lq}}}{\partial t} - S_{\mathrm{lq}} \frac{\partial \varepsilon}{\partial t}\right],$$
$$S_{\mathrm{gz}} \frac{\partial P_{\mathrm{gz}}}{\partial t} = -\frac{K_{\mathrm{gz}}}{\phi}\left[\frac{\partial \zeta_{\mathrm{gz}}}{\partial t} - \phi \frac{\partial S_{\mathrm{gz}}}{\partial t} - S_{\mathrm{lq}} \frac{\partial \varepsilon}{\partial t}\right], \qquad (14)$$

where K_{lq},K_{gz} are liquid and gas bulk modules.

3.4. Comparison of results

Fig. 5 and Fig. 6 compare the temperature results by five models, at r = 0.685 and 1.45 m, respectively. The calculated and measured values agree well and demonstrate that conductive heat transfer is the main heat transport mechanism. All models correctly reproduced the temperature behaviour during the complete heating–cooling phases, and the reasons for the discrepancies are most likely the differences in model geometry, mesh size, moisture–heat interaction models with different thermal diffusion laws and values of thermal diffusivities.

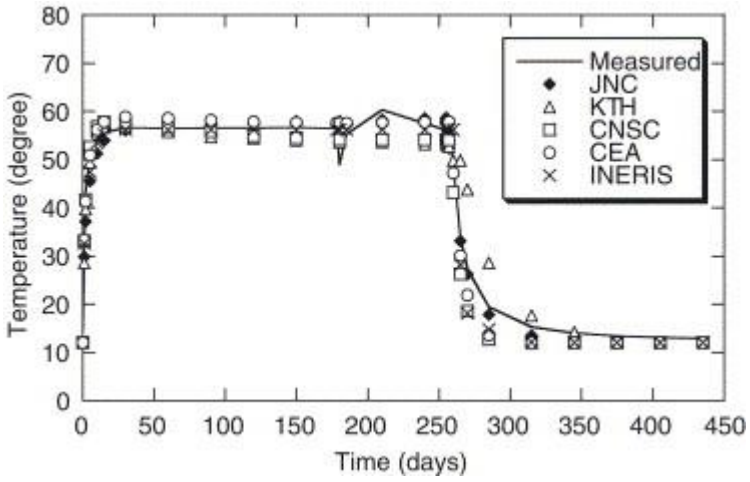

Fig. 5. Time histories of temperature at r = 0.685 m.

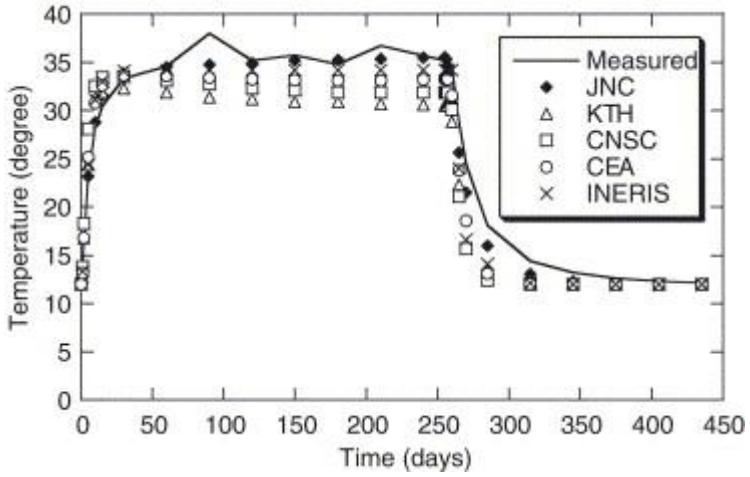

Fig. 6. Time histories of temperature at r = 1.45 m.

Fig. 7, Fig. 8 and Fig. 9 compare the water contents at r=0.54, 0.685 and 0.85 m, respectively, as functions of time during both heating and cooling periods. The calculated results agree well with the measured ones at r = 0.54 and 0.85 m, both qualitatively and quantitatively, for all teams except the INERIS/ANDRA model, which may be caused mainly by the treatment of steel of the canister as a porous medium and the fact that the thermally driven water transport was ignored in the INERIS/ANDRA model. The major discrepancies exist at in all models except for the KTH/SKI model. The possible causes for such major discrepancies could be many, especially coupled porosity–permeability models, which were ignored in all models, and condensation–evaporation coupling effects, which were ignored in CEA/IRSN, CNSC, JNC and INERIS/ANDRA models.

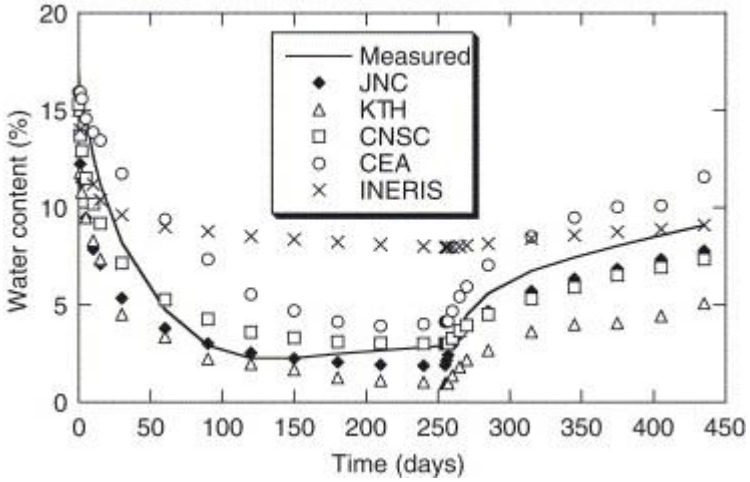

Fig. 7. Water contents at r = 0.54 m.

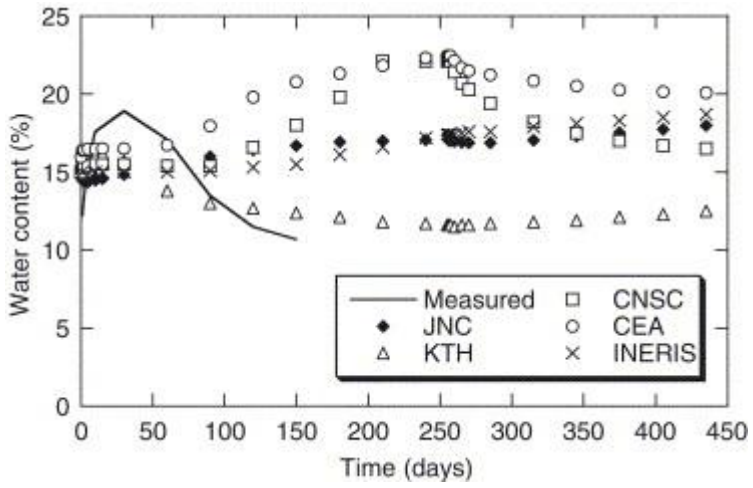

Fig. 8. Water contents at r = 0.685 m.

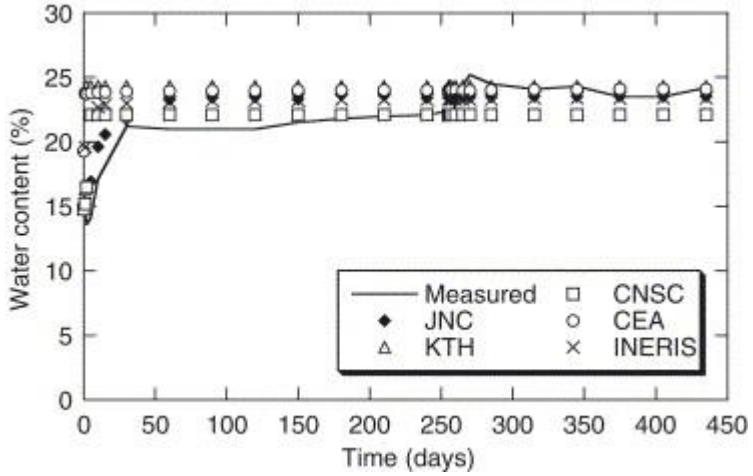

Fig. 9. Water contents at r = 0.85 m.

Fig. 10 compares the radial stress at as a function of time, where experimental data are available. For the CEA/IRSN, CNSC, KTH/SKI and JNC models, although large discrepancies still exist, the general trend among the models agrees fairly well with the measured data at this point. This indicates that the thermal expansion phenomenon is modelled fairly well by these teams, but not the swelling process, which may be the reason for the discrepancies.

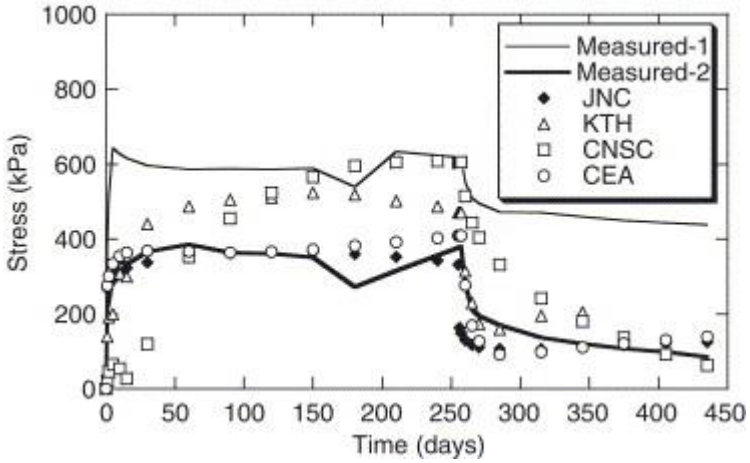

Fig. 10. Radial stress at r = 0.54 m.

Fig. 11 and Fig. 12 compare radial strains at r = 0.685 and 1.45 m, respectively. Although large discrepancies still exist among the models, a consistent trend can still be detected between the measured and calculated strains at . At in the rock, the JNC results of the strain is consistent with the experimental data in trend; CNSC model results were under-predicted, due to the fixed outside boundary that is too close to the centre (radial distance of 3 m).

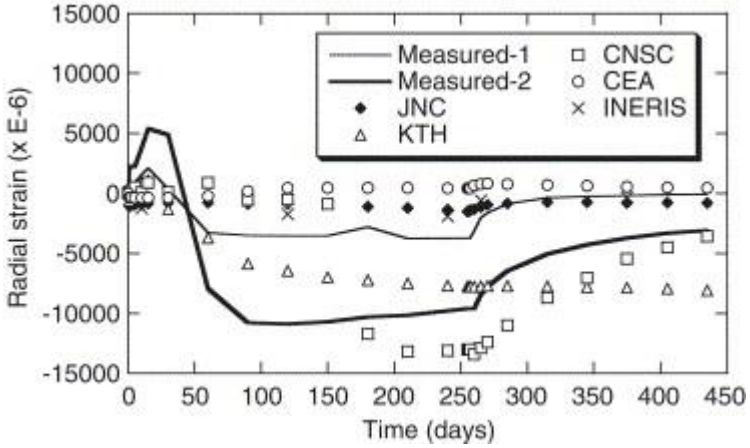

Fig. 11. Radial strains at r = 0.685 m.

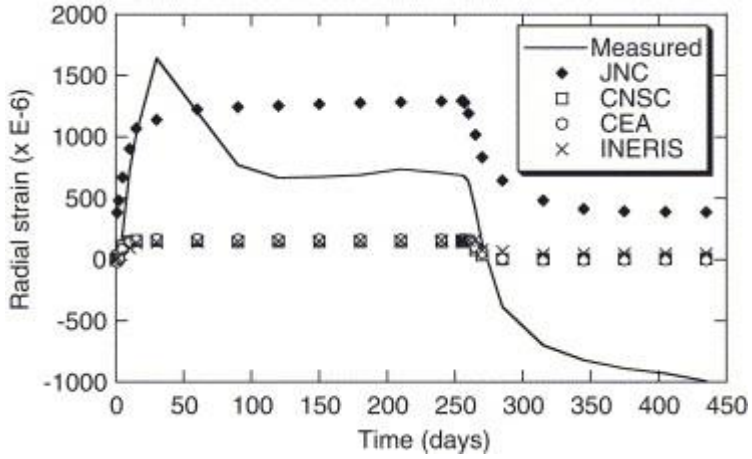

Fig. 12. Radial strains at r = 1.45 m.

3.5. Summary

A simplified axisymmetric model of the in situ THM experiment at the Kamaishi mine was simulated by five different numerical models. Although the model geometry is much simplified compared to the field test conditions, improved simulations of the general THM responses were obtained as compared to previous blind predictions performed within the DECOVALEX II project. The measures taken for improvement were the following:

• Parameter improvements (reduced rock mass permeability and rock mass thermal expansion by the KTH/SKI team, and increased thermal expansion coefficient and reduced swelling pressure constant of the buffer by the JNC team).

• Inclusion of the sealing of rock fractures by penetrating bentonite by the KTH/SKI team, which can explain the uniform (axisymmetric) wetting of the bentonite.

• An improved swelling/shrinking strain function combined with an increased thermal expansion of the bentonite giving a good match of the mechanical (stress, strain) behaviour of the buffer by the KTH/SKI team.

• Use of higher E (Young's modulus) and ν (Poisson's ratio) of the bentonite near the heater, and use of a “sealed” layer of rock around the bentonite by the CNSC team.

As a result of the above measures, the results from the simplified axisymmetric model used in the re-evaluation of the THM experiment at the Kamaishi mine showed general improvement over the original models used in the prediction phase during the DECOVALEX II project. In general, the mechanical behaviour of the buffer is complex with forces contributing from shrinking/swelling in all parts of the bentonite, external stress from the thermal expansion of the heater and rock, and internal thermal expansion of the bentonite itself. However, a reasonable prediction of the mechanical behaviour can be made only if all relevant bentonite properties are known from laboratory tests.

4. Scoping calculations for the near-field

The models that are used in the calibration of the Kamaishi THM experiment are used to perform scoping calculations of the near-field of a hypothetical repository. The definition of the scoping calculation is given in this section.

From the conceptual design of the repository as shown in Fig. 3, and assuming repetitive symmetry, one web of the system, comprising one borehole, and a slice of rock and backfill as shown in Fig. 13 are considered.

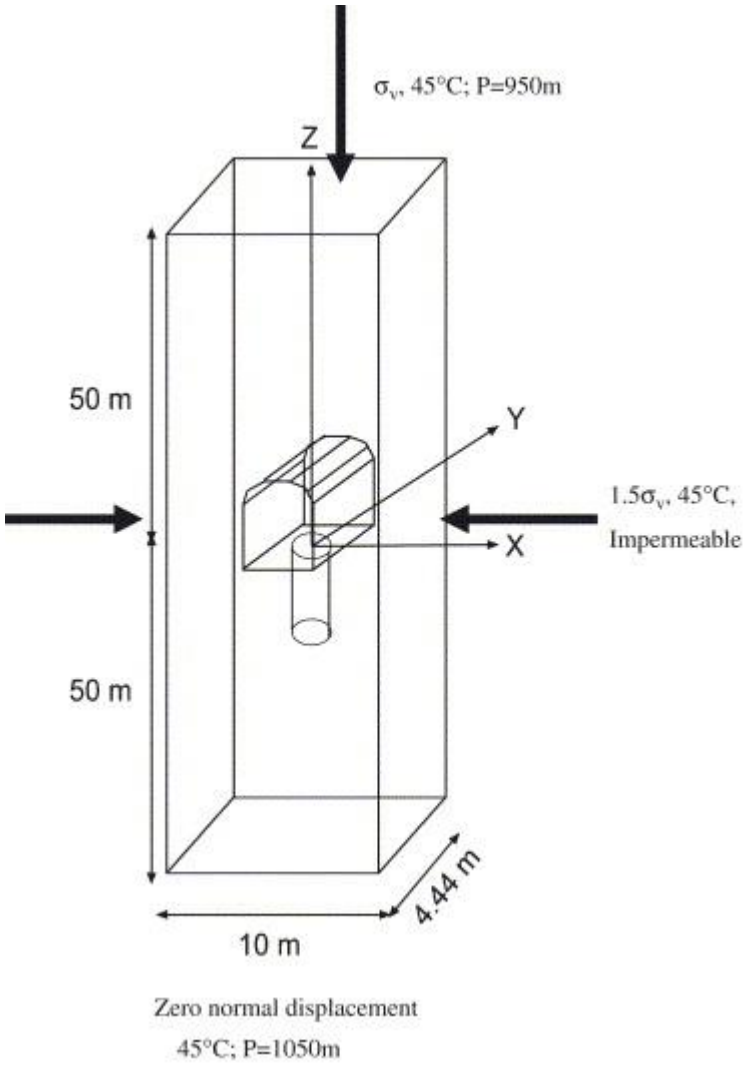

Fig. 13. Conceptual representation of repository near-field.

For the rock mass, two main cases were considered:

(i) The rock mass is considered to be continuous (without explicitly presented fractures) and homogeneous. The scoping calculations for this case constituted phase B of BMT1 [1].

(ii) One discrete horizontal fracture intersects the centre of the emplacement borehole. A combination of this horizontal fracture and other intersecting fractures could also be considered. The scoping calculations for this case constituted phase C of BMT1 [2].

4.1. Rock mass properties

Initial rock mass permeability values of 10^{-18}, 10^{-17} and 10^{-19} m^2 were considered by the research teams, with the median value of 10^{-18} defined as the base case. Additionally, the rock mass permeability was assumed to vary with the effective porosity according to the following function:

$$K = 2.186\times10^{-10}\times n^3 - 5.8155\times10^{-18}, \qquad (15)$$

where K is the intrinsic permeability (m^2) and n is the effective porosity.

Eq. (15), illustrated in Fig. 14, is derived from experimental data obtained from the sparsely fractured rock of the Canadian Shield [10], with a permeability range between 10^{-19} m^2 and 10^{-17} m^2.

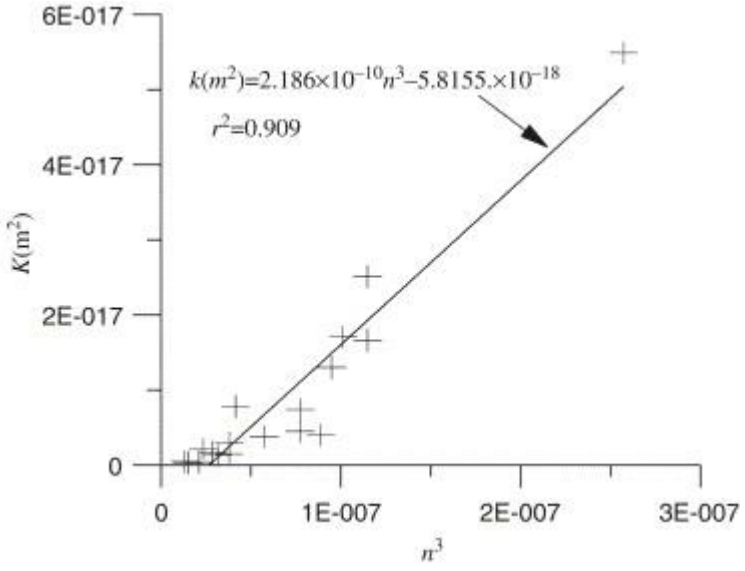

Fig. 14. Permeability–porosity function for rock mass.

The rock mass failure is assumed to be governed by Hoek and Brown's criterion:

$$\sigma'_{1f} = \sigma'_1 - \sigma'_3 - (m\sigma_c\sigma'_3 + s\sigma_c^2)^{0.5}, \qquad (16)$$

where are, respectively, the major effective principal stress at failure, the major effective principal stress and the minor effective principal stress, respectively. Symbols m=17.5 and s=0.19 are empirical constants typical of the granitic rock of the Canadian Shield [11]; σ_c is the uniaxial compressive strength of intact rock samples.

4.2. Analysis sequence

For both phases B and C, the research teams performed the following sequence of simulation:

(i) Firstly, determine the effects of excavation by performing a steady-state analysis, with the boundary conditions as illustrated in Fig. 13. The output of this analysis consists of the distribution of temperature, pore pressure, permeability and factor of safety for rock mass failure. The ambient temperature of 45 °C is consistent with Japanese thermal conditions at a depth of 1000 m. A temperature of 20 °C is assumed inside the tunnel in order to simulate cooling.

(ii) Secondly, perform transient analyses assuming that the buffer, backfill and heater are emplaced instantaneously at time t=0. The analysis shall be conducted for a period of at least 100 years. The results from the steady-state analysis for excavation effects for temperature, stresses and pore pressure in the rock mass would be used as initial conditions. For the buffer and backfill, the initial stresses were assumed to be zero, the initial temperature 20 °C and the initial water content is 15 %. The heat output from the waste is shown in Fig. 15 and is representative of Japanese spent fuel [3]. The boundary conditions for the transient analysis are similar to the ones during excavation, except for the lateral boundaries, where zero normal displacement was imposed to simulate periodic symmetry conditions. The time evolution of temperature, water content and total stresses in the bentonite would be calculated at specific points. In the rock mass, the distribution of temperature, pore pressure, factor of safety against failure and permeability are required at specific times.

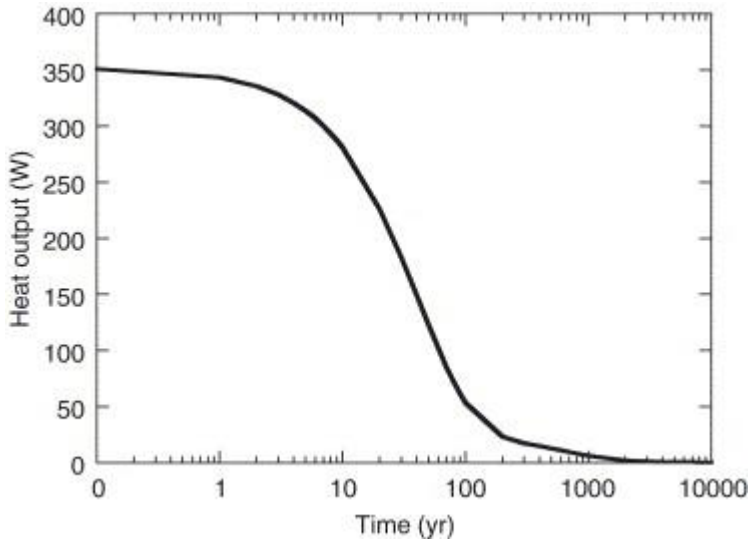

Fig. 15. Heat output from waste canister.

4.3. Evaluation of coupling effects

For both the excavation phase, and the long-term phase with emplaced buffer, backfill and heater, the analyses shall be performed with increasing degree of complexity of coupling [1] and [2]. A comparison matrix will be established in order to compare the implications of various orders of complexity of the coupling, as shown in Table 2.

Table 2. Comparison of output for different degrees of T–H–M coupling

Output	Coupling			
	THM	**TH**	**TM**	**HM**
Temperature				NA[a]
Water content			NA	
Pore pressure			NA	
Stress/safety factor		NA		
Permeability		NA		

[a] NA: not applicable.

The above numerical simulations and results are presented in the two companion papers about BMT1 [1] and [2].

5. Results, comparison and concluding remarks

In this paper, we provided the rationale and definition of a benchmark test called BMT1 to look at the implications of THM couplings on safety parameters in the near-field of a hypothetical repository. This hypothetical repository possesses composite features since it is based on a Japanese design, with a Japanese bentonite used as buffer material and the heat output characteristics of Japanese spent fuel. However, the permeability and strength characteristics of the rock mass are based on typical properties of granites of the Canadian Shield.

In Phase A of BMT1, the T–H–M models used by the research teams are calibrated against the measured THM output of an in situ heater experiment. All models could reasonably simulate the fundamental physical phenomena, with thermal output being best simulated and swelling stress in the bentonite being the most difficult parameter to simulate. This phase is an important step of conceptualization and characterization of the bentonite and rocks, with the support of an in situ THM experiment, for the confidence building of the models and codes that were applied in phases B and C.

In phase B, the research teams used the T–H–M models to perform scoping calculations for a repository in a continuous and homogeneous rock mass. The results of phase B are reported in detail in a companion paper [1]. The main conclusions of phase B are as follows. The fully coupled THM analysis predicted localized rock mass failure and also important features related to the buffer/backfill resaturation, the rock mass permeability evolution and the swelling stress development in the buffer, which might be overlooked by more simple analyses. The effects of coupling on the above features seem to be amplified when the rock mass permeability is lower. Temperature is the only output parameter that is not significantly influenced by coupling.

In Phase C, the research teams performed calculations with one or several water-bearing discrete fractures intersecting the repository. The results of phase C are reported in detail in a companion paper [2]. The main conclusions of phase C are as follows. As in phase B, the temperature field shows nearly no difference between THM, TH, TM calculations and is very similar to the one in phase B. The fracture(s) accelerates the resaturation of the buffer/backfill and prevents the desaturation of the rock mass. From a mechanical point of view, the fracture(s) constitutes a zone of weakness and results in a more extended zone of damage as compared to the continuous scenario. TH or THM calculations produce very similar pore pressure fields. With respect to the stresses in the buffer, the conclusions are similar to the continuous case, with a predominant effect of pore pressure on total stresses, compared to the thermal stresses.

From the results of the BMT1 works, it appears that from a technical point of view the effect of coupling will be either short lived (several decades to 100 years) and will not impact long-term (thousands to hundreds of thousand years) safety issues, or could be rectified by adequate design and operation methodology (e.g. avoid over-cooling the galleries). The influence of the host rock properties (e.g. permeability) on the long-term safety seems to be much more important than coupling, since one has much less control over these properties. However, the short-term period, where coupled processes are important, corresponds to the construction, operation and pre-closure monitoring periods for most disposal systems. This period is crucial for repository design and construction, confidence building, demonstration purposes and public acceptance. In order to interpret and assess the monitoring data collected during that pre-closure period, a fully coupled approach is necessary for PA analyses.

Acknowledgement

The authors sincerely thank the funding organization, ANDRA, BGR, CNSC, IRSN, JNC and SKI for their financial support and all participants of DECOVALEX III project for very useful feedbacks on the work presented in this paper.

References

[1] A. Millard, A. Rejeb, M. Chijimatsu, L. Jing, J. De Jonge, M. Kohlmeier, T.S. Nguyen, J. Rutqvist, M. Souley and Y. Sugita, Numerical study of the THM effects on the near-field safety of a hypothetical nuclear waste repository—BMT1 of the DECOVALEX III project. Part 2: effects of THM coupling in continuous and homogeneous rocks, Int J Rock Mech Min Sci (2005).

[2] J. Rutqvist, M. Chijimatsu, L. Jing, A. Millard, T.S. Nguyen, A. Rejeb, Y. Sugita and C-F. Tsang, Numerical study of THM effects on the near-field safety of a hypothetical nuclear waste repository—BMT1 of the DECOVALEX III Project. Part 3: effects of THM coupling in sparsely fractured rocks, Int J Rock Mech Min Sci (2005).

[3] Japan Nuclear Cycle Development Institute. Second progress report on research and development for the geological disposal of HLW in Japan, H12: project to establish the scientific and technical basis for HLW disposal in Japan. Project overview report, JNC TN1410 2000-001, 2000.

[4] Power Reactor and Nuclear Fuel Development Corporation. Kamaishi International Workshop Proceedings, PNC TN7413 98-023, 1998.

[5] M. Chijimatsu, T. Fujita, Y. Sugita, K. Amemiya and A. Kobayashi, Field experiment, results and THM behavior in the Kamaishi mine experiment, Int J Rock Mech Min Sci 38 (2001) (1), pp. 67–78.

[6] Fujita T, Chijimatsu M, Ishikawa H, Suzuki H, Matsumoto K. Coupled thermo-hydro-mechanical experiment at Kamaishi mine. Technical Note 11-96-04, Fundamental properties of bentonite OT-9607, PNC TN8410 97-071, Power Reactor and Nuclear Fuel Development Corporation, 1997.

[7] J. Rutqvist, J. Börgesson, M. Chijimatsu, A. Kobayashi, L. Jing, T.S. Nguyen, J. Noorishad and F. Tsang C-, Thermohydromechanics of partially saturated geological media: governing equations and formulation of four finite element models, Int J Rock Mech Min Sci 38 (2001) (1), pp. 105–128.

[8] J. Rutqvist, J. Börgesson, M. Chijimatsu, T.S. Nguyen, L. Jing, J. Noorishad and C.-F. Tsang, Coupled thermo-hydro-mechanical analysis of a heater test in fractured rock and bentonite at Kamaishi mine–comparison of field results to predictions of four finite element codes, Int J Rock Mech Min Sci 38 (2001) (1), pp. 129–142.

[9] Verpeaux P, Millard A, Charras T, Combescure A. A modern approach of large computer codes for structural analysis. Proceedings of the SMIRT 10th Conference, Los Angels, USA, 1989.

[10] T.J. Katsube and D.C. Kamineni, Effect of alteration on pore structure of crystalline rocks: core samples from Atikokan, Ontario, Can Mineral 21 (1983), pp. 637–646.

[11] Atomic Energy of Canada Ltd, Used fuel disposal centre—a reference concept, AECL Whiteshell, Pinawa, Manitoba, Canada (1992).